ELSEVIER

Biochimica et Biophysica Acta 1330 (1997) 145–156

BIOCHIMICA ET BIOPHYSICA ACTA
BBA

Effect of lithium and sodium ions on a charged membrane of dipalmitoylphosphatidylserine: a study by molecular dynamics simulation

J.J. López Cascales, J. García de la Torre *

Departamento de Química Física, Universidad de Murcia, Campus de Espinardo, 30071, Murcia, Spain

Received 11 June 1997; accepted 27 June 1997

Abstract

We describe a series of molecular dynamics simulations performed on a model of charged lipid bilayer (dipalmitoylphosphatidylserine) and water, in presence of sodium and lithium ions, with an atomic detail. The structure of the lipid membranes was strongly affected by the presence of lithium, as manifested by the observation of a transition from a disordered to a gel state. Concerning the mechanism of such a transition, it was associated to the dehydration that we detected in the lipid–water interface in the presence of lithium. This dehydration introduced an increase in the lipid–lipid interactions, and as a consequence, a diminution of the disorder of the membrane. When both types of ions are present in the aqueous phase, lithium shown a special affinity for the lipid membrane displacing almost all the sodium ions toward the middle of the water layer. As a result, we observed remarkable differences in the atom and electric field distributions across the lipid membrane. Concerning the diffusion and orientation of water molecules across the lipid–water interface, we also observed a strong dependency of the type ion. On the other hand, the mobility and the hydration shell of lithium and sodium ions are strongly perturbed by the presence of the charged lipid bilayer. The lipid layer was responsible for a dehydration of the ions compared to bulk water. This dehydration was compensated by an increase of coordination number of the ions with the lipid oxygens. Also, the residence times of water in the first hydration shell of lithium and sodium ions are perturbed by the presence of the lipid membrane. © 1997 Elsevier Science B.V.

Keywords: Charged bilayer; Structure; Dynamics; Lipid; Alkaline ion; Water; Electric potential

1. Introduction

The study of lipid bilayers is of a crucial importance in understanding the role played by the lipids in biological membranes. The bilayers control the diffusion of small molecules, water and ions through biological membranes and also afford a suitable environment to some molecules embedded in the membrane, such as proteins, carbohydrates, etc.

Specifically, the structure and behaviour of lipid layers are dramatically affected by the pH, ionic strength and type of ions in solution [1–3]. Thus, most lipids show a similar behaviour in the presence of alkaline ions, with the well known exception of lithium [3], which introduces important modifications in PS (PhosphatidylSerine) membranes. Small con-

* Corresponding author. Fax: +34-68-364148; E-mail: jgt@fcu.um.es

PII S0005-2736(97)00156-9

centrations of lithium perturb the lipid state, and increase the critical temperature [3], changing the membrane structure from a disordered state to a gel one.

The study of the effects of lithium on membranes containing serine has another importance, due to its therapeutical properties in the treatment of some mental diseases, such as manic depressive illness [3]. In fact, the interaction of this ion with membranes containing PS (the principal lipid of nervous cells), structurally changes the membranes of such cells, and modify their activity [4]. Although, the routes by which Li can enter and leave cells have not been adequately defined, it has been suggested that in excitable cells, Li can enter through voltage-dependent Na channels [5].

The study of all these processes from an experimental point of view presents certain obstacles, mainly associated to the structural characteristics of the system. In this regard, molecular dynamics simulations has been widely accepted as an important biochemical tool, since it affords valuable information regarding the dynamic and steady properties of the system, such as diffusion coefficients, electric potential across the membrane, an evaluation of the lipid–water interface, etc. [6–10].

Based on our and other's growing experience in the field of MD simulations of biological membranes [10–15], in the present work we study at atomic level the effect of different concentrations of lithium ions on a DPPS (dipalmitoylphosphatidylserine) membrane. In addition, we study the behaviour of sodium and lithium ions in the aqueous region when they approach a charged membrane.

2. Experimental

2.1. Setting up the system

A periodical three-dimensional box was generated as follows: Two lipid layers of 32 lipids each were generated by copying a single molecule of $DPPS^-$ (Fig. 1), which was built by using the commercial package HyperChem [16]. Next, a 1 nm thick layer of water molecules was confined between the two lipid layers by copying an equilibrated box containing 216 water molecules of the SPC [17] model. A total

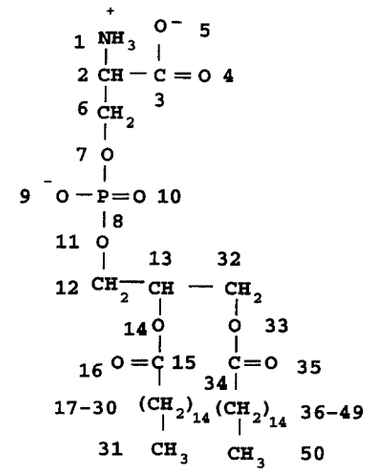

Fig. 1. Dipalmitoylphosphatidylserine molecule, $DPPS^-$.

number of 732 water molecules were required to fill such a gap. Due to the net charge on the $DPPS^-$ lipid molecules, the system was neutralized by the addition of counterions, substituting 64 water molecules by 64 counterions. In a first step, 64 water molecules were substituted by sodium ions (case A), following the criterion of minimum electrostatic energy. Next, two other systems, in which sodium ions were completely (case B) and partially (case C) substituted by lithium ions, were generated. Three snapshots corresponding to the three membranes mentioned above are displayed in Figs. 2–4.

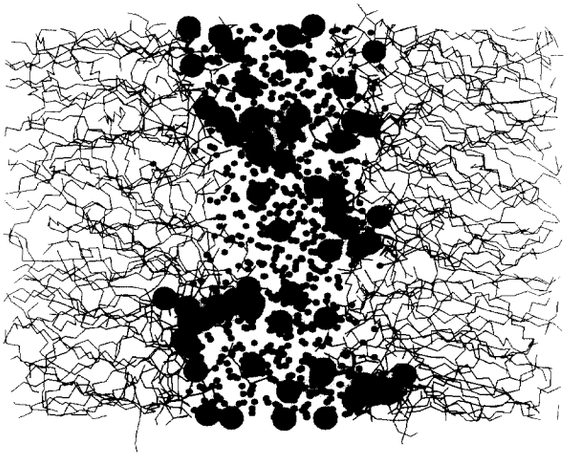

Fig. 2. Snapshot of a $DPPS^-$ membrane along the trajectory containing 64 Na^+. Sodium ions are represented by big spheres and water by the small ones.

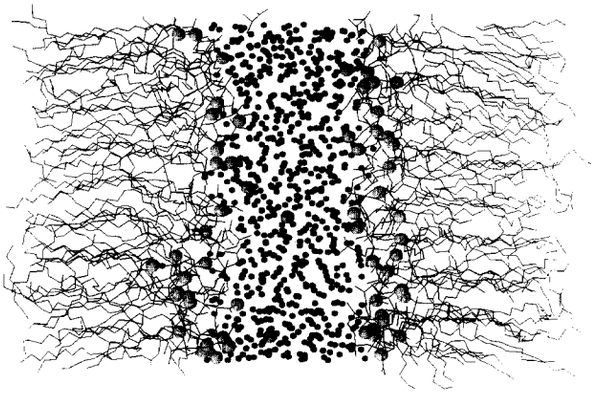

Fig. 3. Snapshot of a $DPPS^-$ membrane along the trajectory containing 64 Li^+. Lithium ions are represented by big spheres and water by the small ones.

The atomic charge distribution on each atom of a lipid molecule was calculated by means of the CNDO quantum mechanical method [18], as in previous articles [14,15]. During MD simulation, all charges were halved (except for the SPC water model) in order to reduce the poor screening arising from the introduction of SPC water molecules between adjacent lipids. For further information, we address the readers to previous articles [14,15,19].

When the structure of the whole membrane has been generated, it was submitted to steepest descent energy minimization, in order to remove unwanted

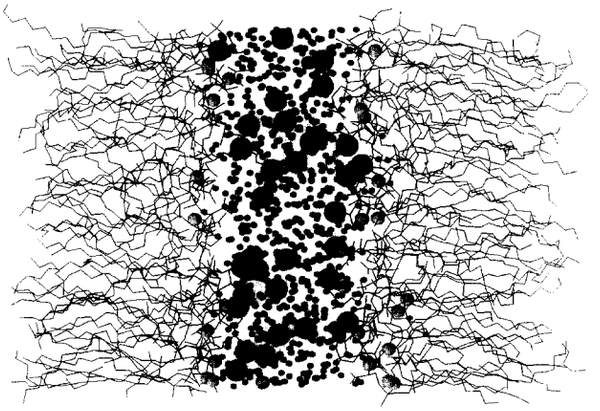

Fig. 4. Snapshot of a $DPPS^-$ membrane along the trajectory containing 32 $Na^+ + 32$ Li^+. Sodium ions are represented by the big spheres, lithium by the medium ones and water by the smallest ones.

contacts between adjacent atoms. GROMOS [20] was the force field employed in our simulations. Lennard–Jones and dihedral parameters were taken from previous works [19]. The Ryckaert–Bellemans potential [21] was used along the alkane chains instead of standard GROMOS parameters, because this force field reproduces the *cis–trans* statistics along alkane chains more accurately than the GROMOS force field. The Lennard–Jones parameters of lithium ions were taken from the literature [22].

During the whole simulation, a time step of 2 fs was used. Bond lengths were constrained by SHAKE [23], with a tolerance constant of 0.0001 nm. Two different spherical cut-offs were employed, as in previous works by Berendsen and coworkers [7,13–15]: a short cut-off of 0.8 nm and a long spherical cut-off of 1.7 nm. We are aware of the critical influence of this parameter on the dynamic and stationary properties of ions and water, as described by Stouch et al. in a previous article [24]. The neighbour list between non-bound atoms was updated every 10 time steps.

The system was coupled to a temperature bath [25] at 350 K (well above the transition temperature of 326 K [26] in the absence of lithium ions), and a pressure bath of 1 atm [25] with coupling constants of $\tau_T = 0.1$ and $\tau_P = 0.5$ ps.

Under these conditions, three different simulations were carried out in which: (A) 64 sodium ions were employed as counterions. In this case, 360 ps were performed and discarded from the analysis during the equilibration of the system, followed by another 200 ps that were used in the analysis. (B) Only lithium ions were used as counterions. In this case, all the sodium ions of the first simulation were substituted by lithium ions, and 150 ps were performed during the equilibration, followed of 200 ps which were employed in the analysis. (C) 32 sodium ions of case A were randomly substituted by 32 lithium ions. The first 150 ps were discarded during the equilibration of the system and the analysis was performed over the following 200 ps. In all three cases, the volume of the computing box was the parameter used to decide that the system had stabilized. The dimensions of the box (in nm) were the following: (A) $V_x = 4.448 \pm 0.014$, $V_y = 4.03 \pm 0.03$, $V_z = 5.76 \pm 0.04$; (B) $V_x = 3.96 \pm 0.08$, $V_y = 4.16 \pm 0.04$, $V_z = 6.13 \pm 0.12$; (C) $V_x = 4.56 \pm 0.11$, $V_y = 3.70 \pm 0.17$, $V_z = 5.99 \pm 0.09$.

3. Results and discussion

3.1. Membrane structure

In the presence of Na^+ ions (case A), a value of 0.54 ± 0.03 nm^2 emerged from our simulations for the surface area per lipid,which was in good accordance with the 0.50 to 0.55 nm^2 measured in different experimental conditions [2,27]. In case C, a value of 0.527 ± 0.013 nm^2 was obtained and 0.51 ± 0.06 nm^2 in case B. These results agree with experimental data [3] in which a reduction of the surface area per lipid was observed in the presence of LiCl, this effect being much more noticeable at higher lithium concentrations in solution.

Such a reduction in the surface area per lipid in the presence of lithium ions meant that an increase the order parameter along the ethylene chains was to be expected [28]. Fig. 5 displays the deuterium order parameter $-S_{CD}$ averaged over the two lipid tails in the presence and absence of lithium ions. From the simulated trajectory, $-S_{CD}$ is obtained as follows:

$$S_{CD} = \frac{2S_{xx}}{3} + \frac{S_{yy}}{3} \quad (1)$$

where x-, y- and z-axes are taken with respect to the plane defined by the H–C–H atoms of the ethylene lipid tails [14]. Fig. 5 shows the good agreement between the experimental and simulation results in the absence of lithium. When sodium ions are partially or completely substituted by lithium ions, we observe an increase in the order parameter along the tails, which corresponds to the transition from a disordered to a gel state. We should point out that neither from the discrete time nor from the size of our simulations, we can obtain concluding results about membrane phase transitions, from our simulations we only observe a tendency from a disordered state to a more ordered state. The increased order in the phospholipid tails can also be appreciated by comparing the snapshots in Figs. 2 and 3. In Fig. 5, we see that the results for 32 Na^+ + 32 Li^+ nearly coincide with those for 64 Li^+. Thus, the effect of substituting Na^+ by Li^+ is nearly the same when only half of the ions are substituted, which is in agreement with experimental observations [3] that lithium ions perturb the conformation of the lipids at a wide range of concentrations, by inducing more order in their tails.

As regards, the *cis–trans* conformation rate along the tails, Fig. 6 shows how in the absence of lithium, the percentage of *trans* conformations always remain below 75%, which corresponds to a disordered state. The presence of lithium ions on the other hand, increases the rate to above 80%, typical of a gel state.

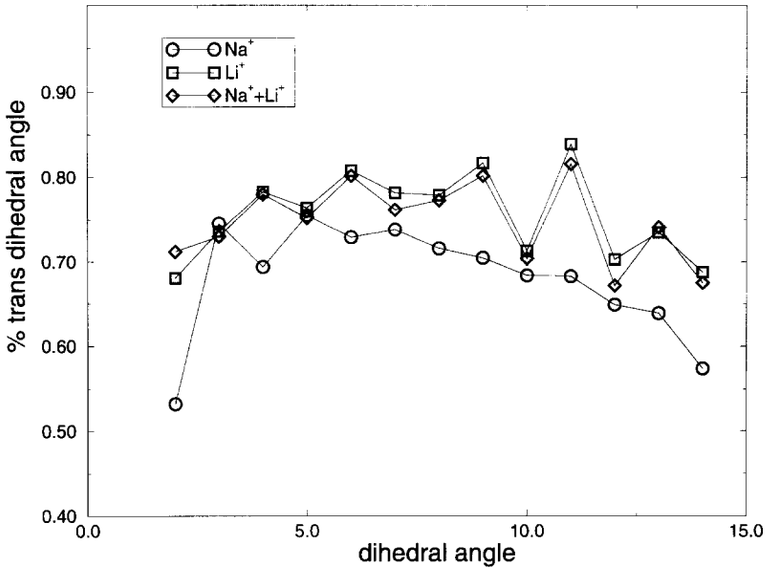

Fig. 5. Order parameter along the alkane lipid chains averaged over both tails.

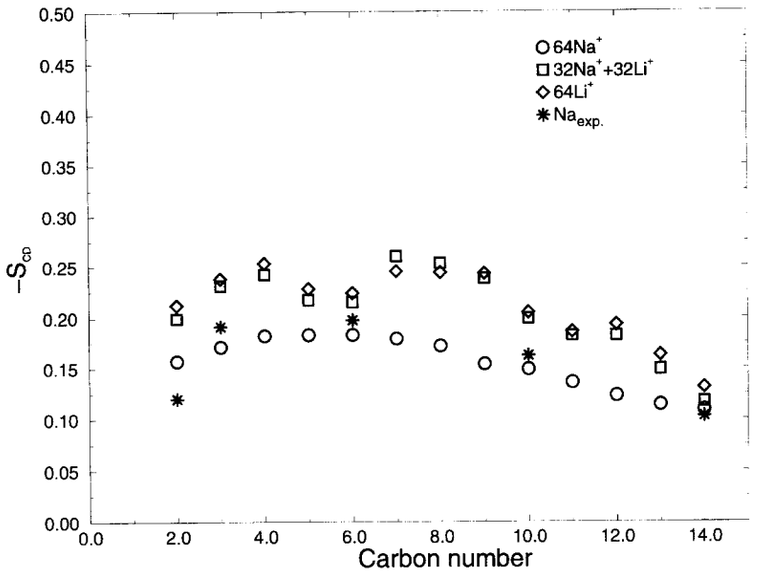

Fig. 6. *Cis–trans* ratios along the alkane lipid chains averaged over both tails.

3.2. Atom distribution

Fig. 7 displays the atom distribution (in atoms nm^{-3}) across the membrane in the presence and absence of lithium, and it is clear how the distribution profiles are strongly perturbed by the presence of lithium. Fig. 7a (no-lithium) displays an almost uniform distribution of sodium ions across the water layer, with the exception of a slight increase in the vicinity of the lipid heads. Neither water molecules nor sodium ions penetrated in the core of the hydrocarbon region.

In the presence of only lithium ions (Fig. 7b), qualitative differences were evident from our simulations compared to the situation represented by Fig. 7a. First, as the lithium distribution fell to almost zero in the middle of the water layer, there was a noticeable increase in their concentration in the vicinity of the lipid heads, illustrating the strong affinity of the lithium ions for the lipid heads, in accordance with experimental measurements [3]. Fig. 7c, shows how when only half of the sodium ions were substituted by lithium, sodium ions were almost totally removed from the membrane surface, this region principally being occupied by lithium ions. In other words, there is a clear segregation of the counterions in the Li + Na case, Na^+ preferentially occupying

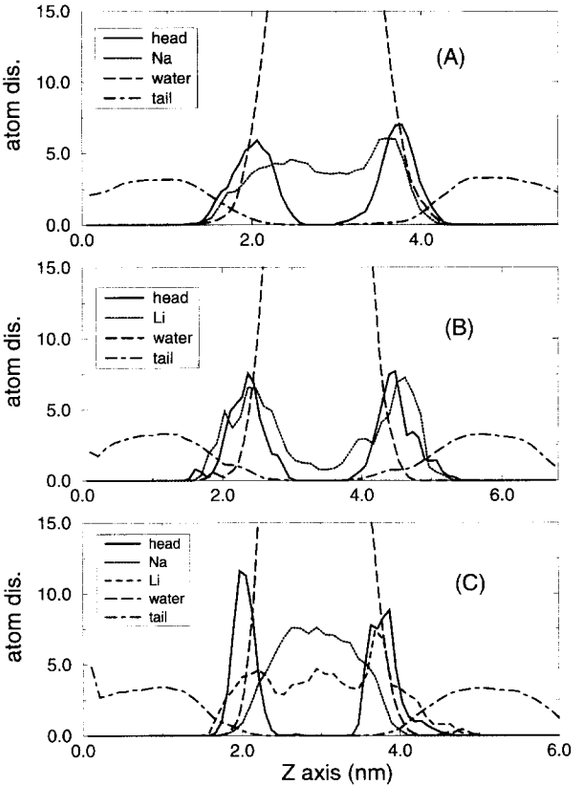

Fig. 7. Atom distribution across the membrane in atom nm^{-3}. (A) in the presence of 64 Na^+. (B) in the presence of 64 Li^+. (C) In the presence of 32 Na^+ and 32 Li^+.

the water region, while Li^+ forms another ionic layers in both lipid-head regions. This partitioning of the counterions into different layers may have important consequences in membrane behaviour. The snapshots in Figs. 2–4 clearly illustrate the different positioning of the two ions.

3.3. Charge and electric field across the membrane

An electric field is obtained across the membrane as a consequence of the distribution of charged atoms, ions and water molecules within it. Fig. 8 displays the charge density distribution (expressed in e nm^{-3}) of the different components across the membrane (from MD simulation, the split charges of each component can be obtained). A comparison of Fig. 8aFig. 8b, leads to the following conclusions: Lithium ions very effectively screen the full charge of the lipid layer and, as a consequence, the surface potential on the membrane is modified with respect to that occurring when lithium is not in solution.

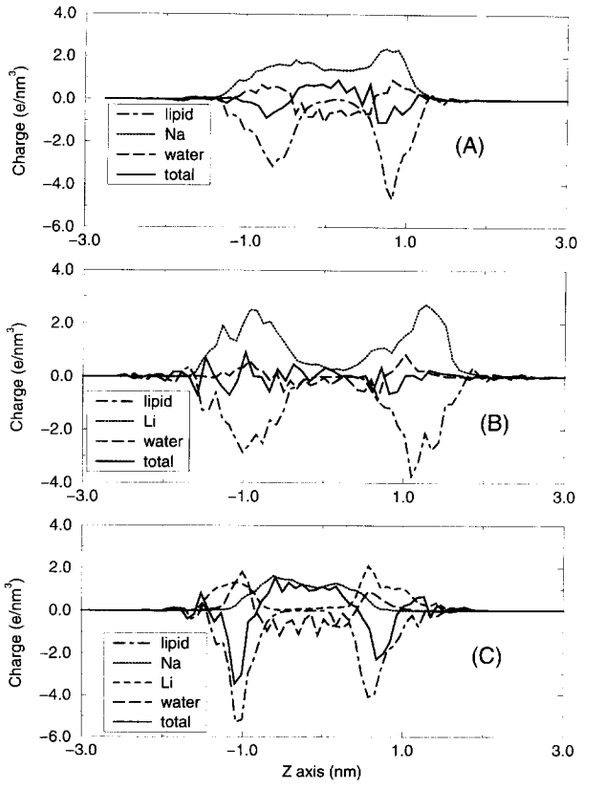

Fig. 8. Charge distribution profiles across the membrane (e nm^{-3}). (A) in the presence of 64 Na^+. (B) in the presence of 64 Li^+. (C) In the presence of 32 Na^+ and 32 Li^+. The z-axis was centred in the middle of the water layer.

Fig. 8c, in which lithium and sodium ions are both present in solution, shows how the lipid charge is only partially compensated by the lithium ions in the interface, while the rest is compensated by the orientation of the dipole of the water molecules, with no contribution from sodium ions at the interface.

From simulation, the electric potential across the membrane can be obtained by means of a double integration of the charge density $\rho(z)$ [7]:

$$\psi(z) - \psi(0) = -\frac{1}{\epsilon_0}\int_0^z dz' \int_0^{z'} \rho(z'')dz'' \qquad (2)$$

where the origin for z was the middle of the lipid layer. Hence, we can split the potential into the separate contributions of its components. Fig. 9 displays the total and the partial electric potential $\psi(z)$ across the membrane.

Fig. 9 also shows that the lipid + counterion contribution to the total potential depends strongly on the type of ion. We can see how lithium ions (Fig. 9a) screen the lipid potential, reaching a value of 2 V in the middle of the water layer against the 6 V in its absence or when both types of ion are present in solution.

Screening of the lipid surface potential by different types of ions has been studied experimentally [2] with the goal of identifying the electrostatic contribution to the temperature of the phase transition made by the phosphatidylglycerol bilayers. The results reported in this article are analogous to the results reported in the mentioned experimental work, in the sense that lithium ions screen the net charge of lipid membranes very effectively.

Regarding the water contribution to the electrostatic potential, Fig. 9b displays the behaviour expected: Water molecules tend to compensate the lipid + counterion potential by means of the water dipole orientation.

Fig. 9c displays the total potential across the water layer. From this, we observe how the shape of the electric potential is strongly dependent on the type of ion in solution. Thus, the electric potential ranges from 0.5 V in the presence of lithium alone to 2.5 V in the presence of lithium + sodium ions or in the absence of lithium.

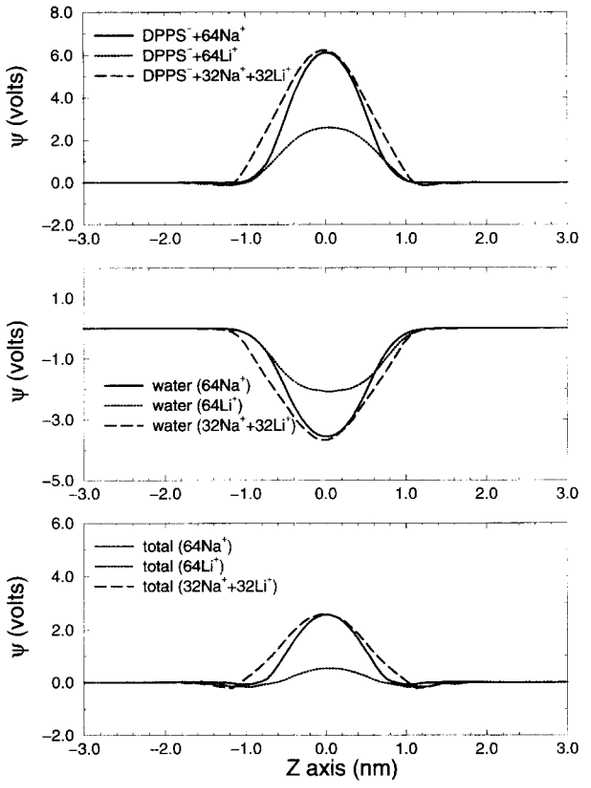

Fig. 9. Electric potential across the membrane in V. (A) Contribution of lipids + counter ions. (B) Contribution of water. (C) Total potential.

From Fig. 9c, we observe that in the presence of lithium ions, the total potential in the middle of the water layer is comparable to the value of 0.5 V obtained for uncharged DPPC membranes [7]. This diminution in potential in the presence of lithium ions clearly reflects to the fact that lithium ions stay anchored to the lipid surface (Fig. 7b), producing in this way a much better screening of the lipid-head charges than in the presence of sodium.

3.4. Lipid–lipid and lipid–ions interaction

One interesting aspect studied in this work has been the plausible effect of lithium and sodium ions on the lipid–lipid interactions.

Fig. 10 displays the radial distribution functions $g(r)$ between serine ammonium groups ($-NH_3^+$) and lipid oxygen atoms of adjacent lipids at different concentrations of lithium ions. The radial distribution function $g(r)$ is defined as follows:

$$g(r) = \frac{N(r)}{4\pi r^2 \rho \delta r} \tag{3}$$

where $N(r)$ is the number of oxygen atoms in a spherical crown between r and $r + \delta r$, r being the distance from the reference atom, and ρ is the number density (taken as the ratio of the total number of atoms to the volume of the computing box).

From Fig. 10, we see how the substitution of all the sodium ions by lithium almost removes the charge interaction between the serine ammonium groups and serine carbonyl oxygens (O_4) of adjacent lipids (according to the atom numeration of Fig. 1). On the other hand, we observe an increase in the strength of the interactions between the serine ammonium group and the phosphatidyl oxygens (O_9). When both

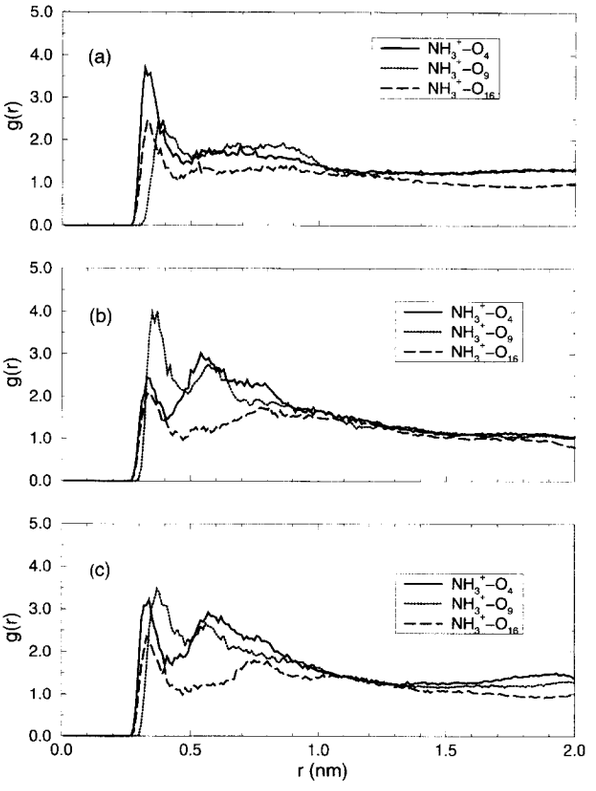

Fig. 10. NH_3^+–O distribution function $g(r)$. (A) in the presence of 64 Na^+. (B) in the presence of 64 Li^+. (C) In the presence of 32 Na^+ and 32 Li^+.

Table 1
Coordination number of lipid oxygens by ions

Oxygen	64 Na	64 Li	32 Na	32 Li
4	0.38	1.12	0.12	0.38
5	0.32	0.82	0.14	0.50
9	0.85	0.82	0.04	0.55
10	0.85	0.81	0.05	0.55
16	0.09	0.19	0.00	0.11
35	0.03	0.09	0.00	0.06

Atom numeration indicated in Fig. 1.

sodium and lithium ions are present in the aqueous phase (Fig. 10c), we observe how the radial distribution functions between ammonium serine group and serine carbonyl (O_4) and phosphatidyl oxygens (O_9) show a similar shape.

Table 1 displays the lithium and sodium coordination numbers around lipid oxygen atoms obtained from our simulations by means of a numerical integration of the first peak obtained in the radial distribution functions. It can be seen how lithium ions tend to coordinate the carbonyl serine oxygen (O_4) instead of the phosphatidyl ones (O_9). Sodium ions behaved in an opposite way in our simulation, since there were located around the phosphatidyl oxygens (O_9).

Combining the results obtained for the lipid–lipid interactions with those obtained for lipid–ion coordination, we observe that the reduction in ammonium–O_4 coordination in the presence of lithium ions is clearly compensated by the coordination with lithium. When both ions are in solution, we observe that lithium ions almost totally displace the sodium ions from the vicinity of the lipid oxygens. From the lipid–lipid and lipid–ion radial distribution functions obtained in our simulations, we observe how the presence of lithium disrupts the existing lipid–lipid interactions, which are substituted by lipid–lithium–lipid interactions. This type of behaviour has also been reported in experimental NMR and X-ray experiments [2].

4. Water structure and dynamics

4.1. Water orientation

Experimental data [2,29,30] and simulation [7,15,31,24,32], have shown how water molecules close to the lipid–water interface possesses their own identity, clearly differentiating this water from bulk water. Its study is in fact of a great interest for a proper understanding of many biological processes such as the diffusion and permeation of small molecules across membranes [33]. However, this be-

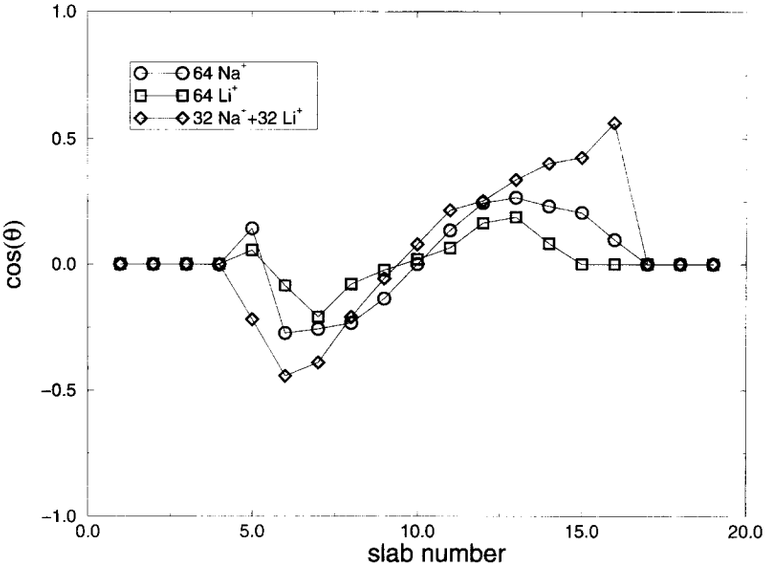

Fig. 11. Cos of the angle formed by the water dipole and the normal to the membrane, in the presence and absence of lithium ions.

haviour greatly depends on the type of lipid head, the ionic strength of the solution, type of ions, etc.

Fig. 11 displays the cosine of the angle formed by the water dipole and the normal to the lipid membrane. In order to study the water dipole orientation across the water layer, the computing boxes of the simulations were divided into 19 slabs and the results are shown in Fig. 11. Angle θ was defined as the angle formed by the unitary water dipole and the z-axis (normal to the lipid interface). Slab number 10 corresponds to the slab centred in the midpoint of the water region.

From Fig. 11, we observe how the presence of lithium ions perturbs the water structure in the proximity of the lipid–water interface, increasing the screening of the electric field across the water layer and, as a consequence, we observe a reduction in the water orientation. In the case of Na^+ alone, the poorer screening of the lipid charge by the sodium ions, introduces a higher orientation in the water molecules and therefore, the water dipole orientation increases in the vicinity of the surface. When sodium and lithium are simultaneously present, we observe that the water molecules reach their maximum value for $\cos\theta$ near the lipid–water interface, with a value of about 0.5 (almost twice the value obtained in the presence of sodium or lithium alone). Again, the effect of Li^+ and Na^+ is greater than for Li and Na alone. This fact is in concord with the trend shown by the electric potential, ψ, in Fig. 9.

For all three cases presented above, a common behaviour was observed: Water molecules orientate their dipoles toward the phospholipid layers, resembling the behaviour previously reported for zwitterionic lipid layers of PE (phosphatidylethanolamine) [9] and PC (phosphatidylcholine) [8,31].

4.2. Lipid layer hydration

As regards lipid hydration, Table 2 displays the values obtained from our simulation by integration over the first hydration shell. From a comparison of the values obtained from our own simulations (in the three systems considered in this paper), we note that lithium ions drastically reduces lipid hydration. These results agree with experimental data obtained by NMR and X-ray measurements [3], where dehydration of PS bilayers was observed in the presence of lithium ions, leading the lipid membranes to a gel state.

Table 2
Coordination number of lipid oxygens and NH_3^+ by water

Oxygen	64 Na	64 Li	32 Na + 32 Li
4	1.98	1.38	1.79
5	1.60	2.04	2.27
9	2.63	1.04	1.36
10	2.63	1.09	1.28
NH_3^+	1.27	0.851	0.816

Atom numeration indicated in Fig. 1.

Hydration of the serine ammonium groups occurs in a similar way to hydration of the lipid oxygens, there being a clear dehydration of this group in the presence of lithium. All these results confirm that lithium brings about a high degree of dehydration, inducing at the same time the ordering of DPPS membranes. Note that the results for 50% Li^+ are close to those for 100% Li^+, indicating that even a small amount of Li may cause an intense dehydration effect.

4.3. Translational diffusion coefficient

Regarding the mobility of water in the vicinity of the membrane interface, the translational diffusion coefficient D_t was computed from our simulations. This quantity is related to its displacement by mean of the Einstein equation,

$$D_t = \frac{1}{2ft}\langle (r(t) - r(0))^2 \rangle \quad (4)$$

in which f is the number of degrees of freedom taken into account in the motion of the particle. From Eq. (4), and a simple linear regression of the square displacement at two different times, we can evaluate D_t. As the motion along the three dimensions of the space does not make sense in this case (the motion of water along the z-axis is constrained by the two lipid layers), we computed the water motion on the pseudo-infinity xy-plane parallel to the membrane. Thus, in Eq. (4), f takes the value of 2. From our simulations, we attempted to estimate the lateral diffusion coefficient $D_{t,xy}$ as a function of the instantaneous z position, in the presence and absence of

Table 3
Translational diffusion coefficient of water expressed as $D_{t,xy} \times 10^5$ cm^2 s^{-1} in different parallel slabs

Slab	64 Na	64 Li	32 Na + 32 Li
6	2.49 ± 0.09	–	1.31 ± 0.03
7	4.0 ± 0.3	2.49 ± 0.03	4.75 ± 0.11
8	5.39 ± 0.06	6.01 ± 0.02	6.18 ± 0.03
9	7.341 ± 0.019	9.27 ± 0.03	6.68 ± 0.02
10	8.170 ± 0.015	10.38 ± 0.05	7.000 ± 0.014

Slab number 10 corresponds to middle of the water layer. Only the first half of the membrane was displayed for symmetry.

lithium. For this, the membrane (cases A, B, C of Section 2.1) was divided into 19 slabs. The high mobility of the water molecules means that they remain very briefly in each slab, and this makes it difficult to assign them to individual slabs. In previous articles [7,14,15] this problem was solved as follows: the trajectory was split into shorter sub-trajectories of 10 ps. On each sub-trajectory, a water molecule was assigned to the particular slab in which its centre of mass (computed along the sub-trajectory) remained during most of the time.

Table 3 shows the computed results of the diffusion coefficients of water in parallel slabs of the membrane, expressed in cm^2 s^{-1}. Slab number 10 was located in the middle of water layer. An important conclusion can be drawn from these results,: the presence of lithium slows down the diffusion of water at the interface (slabs numbered 6, 7, and 8). However, an opposite behaviour was observed in the middle of the water layer, which can be explained as follows: The presence of lithium ions dehydrates the membrane (as discussed above) and the few water molecules that penetrate into the lipid layers behave much more like coordination water than free water. As a consequence, a reduction in the translational diffusion coefficient of the water is to be expected, which is indeed shown by our results.

However, in all the cases described above, we note that the water diffusion coefficient in the middle of the water layer (slabs 9 and 10) agrees with the diffusion coefficient of water at 349 K of 7.5×10^{-5}, for bulk SPC [34], except in the case of lithium alone, when we obtained a value slightly higher than expected.

5. Structure and dynamics of lithium and sodium ions

To date, most of the previous investigations regarding sodium and lithium ions in aqueous solution [35–40] have been carried out without taking into account the presence of a charged diffuse interface, such as the lipid–water interface. Only studies of lithium and sodium's behaviour under uniform electric fields [22] have been carried out.

For this reason, we studied some properties related to the structure and dynamics of these ions in the presence of a charged membrane of DPPS. Table 4 shows the translational diffusion coefficient $D_{t,xy}$ in different slabs of the membrane (19 in total, although for reasons of symmetry we will take into account only the first half). Slab number 10 corresponds to bulk water. Previous calculations of the diffusion coefficient of lithium and sodium ions [22] at very dilute solutions (in bulk water) reported the following results for $D_{t,xy}$: $0.44 \pm 0.18 \times 10^{-5}$ and $0.52 \pm 0.13 \times 10^{-5}$ (cm^2 s^{-1}) for Li^+ and Na^+, respectively, obtained from MD simulations at a temperature of 298 K, which is rather lower than that of our simulation (350 K). From simulation [39] a diffusion coefficient ($D_{t,xy}$) of 2.0×10^{-5} cm^2 s^{-1} was measured for lithium in bulk water at 368 K (close to our temperature). From a comparison of our results in Table 4 with the values shown above, we note a discrepancy for the central slabs of the water layer by a factor of 3. One possible explanation may be that the diffusion of ions submitted to a net potential along the z-axis perpendicular to the membrane plane

Table 4
Translational diffusion coefficient of lithium and sodium ions, expressed as $D_{t,xy} \times 10^5$ in (cm^2 s^{-1}) in different slabs in the membrane

Slab	64 Na	64 Li	32 Na	32 Li
6	–	0.484 ± 0.010	–	0.661 ± 0.016
7	2.0 ± 1.1	1.212 ± 0.014	–	0.81 ± 0.02
8	4.41 ± 0.06	3.02 ± 0.03	4.69 ± 0.12	3.55 ± 0.15
9	7.80 ± 0.06	–	8.03 ± 0.05	6.4 ± 0.3
10	7.30 ± 0.14	–	7.95 ± 0.04	–

Slab number 10 corresponds to middle of the water layer. Only the first half of the membrane was displayed for symmetry.

Table 5
Hydration numbers and residence times of water surrounding lithium and sodium ions (in the presence of only one kind of ion) in different slabs of the membrane

Slab	Hydration numbers		Residence times (ps)	
	Na	Li	Na	Li
6	1.2	0.2	2.3	8.2
7	2.0	1.0	1.8	3.1
8	3.2	2.6	1.6	2.0
9	4.3	4.3	1.5	1.6
10	4.6	5.1	1.4	1.4

Slab number 10 corresponds to the middle of the water layer. Only the first half of the membrane was displayed for purposes of symmetry.

perturbs their mobility in the midwater layer, this increasing the diffusion coefficient. As commented above, it is very difficult to find Li^+ in the middle of the water layer and so, we cannot report results for lithium diffusivity in that region.

From Table 4, we note how the diffusion coefficient decreases for lithium ions much more than for sodium, as we approach the lipid–water interface (number 6, 7, and 8). This indicates that the interaction between lipids and lithium is stronger than that between lipids and sodium.

Integrating the first peak of the radial distribution function of water around lithium and sodium ions (Eq. (3)), we estimate the hydration numbers of their first shell at different depths in the membrane (Table 5). For lithium ions, we obtained the value of 5.1 in the middle of the water layer, 2.7 at the interface and 0.58 in the deepest zones of the membrane. For sodium ions, we obtained the values 4.6, 2.18 and 0.71 in the same conditions. Our results for the two ions in the middle of the water layer show good agreement with previous results obtained from experimental data or from simulation in bulk water [22,38–40], with values ranging from 4 to 6 water molecules for both lithium and sodium. In addition, we observe how lithium and sodium suffer substantial dehydration inside the membrane, this effect being compensated by interaction with lipid molecules, which afford a favourable environment to stabilize this effect. However, lithium and sodium ions do not dehydrate completely even in the deepest zones inside the membrane.

Significant changes were observed in the residence time of water in the first hydration shell of lithium and sodium ions (Table 5) at different depths in the membrane. These values were computed directly from the time spent by a water molecule in the first hydration shell of an ion. The values measured from our simulations agree with previous results obtained for lithium and sodium ions in aqueous solutions using MD calculations [38]. From these results, we observe the trend of the water molecules to remain attached longer to the ions when they penetrate into the membrane than in the bulk. This effect is even more pronounced for lithium than for sodium. From our understanding, this is not entirely unexpected since the water molecules anchored to an ion inside the membrane have very little freedom of movement and therefore they remain bound to the ions for a longer time.

6. Conclusions

The presence of lithium ions strongly perturbs the lipid structure of a DPPS membrane. These changes are reflected by an increase in the order parameter of the lipid tails, as a clear consequence of the transition from a disordered to a gel state. These changes are clearly related to dehydration of the lipid membranes in the presence of lithium. One consequence of this dehydration is an increase in the lipid–ion–lipid interactions.

From our simulations, it is clear that lithium ions act on the membranes by very effectively screening in their electric potential, the lithium atoms anchoring to the membrane surface and thus removing the hydration water. This screening effect is so strong that the electric potential in the middle of the water layer approaches values very close to those reported for uncharged membranes. In addition, the screening of the lipid charge by lithium ions perturbs the dynamic and steady properties of water to a greater extent than when sodium ions are used as counterions.

As regards lithium and sodium ions, the presence of a charged membrane formed of $DPPS^-$ also perturbs the ion hydration shell, reducing their hydration number in the vicinity of the membrane compared to that of bulk water. Our simulations also showed an

increase in the residence time of water in the first hydration shell of ions in the deepest zones of the membrane.

Acknowledgements

We acknowledge support from grant PB93-1132 from the Dirección General de Investigación Científica y Técnica. Support was also provided by Grant CI1*CT940124 from the European Commission of the European Union. JJLC thanks Spanish Government his financial support through a Contrato de Reincorporación de Doctores y Tecnólogos. We are grateful to J.G. Hernández Cifre for his help in some calculations.

References

[1] A.J. Verkleij, B. De Kruyff, P.H.J. Ververgaert, J.F. Tocanne, L.L.M. Van Deenen, Biochim. Biophys. Acta 339 (1974) 432–437.
[2] G. Cevc, A. Watts, D. Marsh, Biochemistry 20 (1981) 4955–4965.
[3] H. Hauser, G.G. Shipley, Biochemistry 22 (1983) 2171–2178.
[4] P. Delva, C. Pastori, D. Degan, G. Montesi, C. Lechi, A. Steele, A. Lechi, Eur. J. Clin. Invest. 26 (1996) 64–70.
[5] I.F. Gow, D. Ellis, J. Mol. Cell Cardiol. 28 (1996) 299–310.
[6] E. Anibal Disalvo, S., Simon (Ed.), Permeability and Stability of Lipid Bilayers, CRC Press, Boca Raton, 1995.
[7] S.J. Marrink, M. Berkowitz, H.J.C. Berendsen, Langmuir 11 (1993) 3122–3131.
[8] T.R. Stouch, Mol. Simulations 10 (1993) 335–362.
[9] K.V. Damodaran, K.M. Merz, B.P. Gaber, Biochemistry 31 (1993) 7656–7664.
[10] D. Bassolino-Klimas, H.E. Alper, T.R. Stouch, Biochemistry 32 (1993) 12624–12637.
[11] R.M. Venable, Y. Zhang, B.J. Hardy, R.W. Pastor, Science 262 (1993) 223–226.
[12] P. Van der Ploeg, H.J.C. Berendsen, J. Chem. Phys. 76 (1982) 3271–3276.
[13] S.J. Marrink, H.J.C. Berendsen, J. Phys. Chem. 15 (1994) 4155–4168.
[14] J.J. López Cascales, J. García de la Torre, S.J. Marrink, H.J.C. Berendsen, J. Chem. Phys. 7 (1996) 2713–2720.
[15] J.J. López Cascales, H.J.C. Berendsen, J. García de la Torre, J. Phys. Chem. 21 (1996) 8621–8627.
[16] HyperCube, HyperChem, 1992.
[17] H.J.C. Berendsen, J.P.M. Postma, W.F. van Gunsteren, J. Hermans, In: B. Pullman (Ed.), Intermolecular Forces, Reidel, Dordrecht, 1981, p. 331.
[18] J.A. Pople, G.A. Segal, J. Chem. Phys. 44 (1966) 3289.
[19] E. Egberts, S.J. Marrink, H.J.C. Berendsen, Eur. Biophys. J. 22 (1994) 423–436.
[20] W.F. van Gunsteren, H.J.C. Berendsen, GROMOS: GROningen MOlecular Simulation, Biomos, Groningen, The Netherlands, 1987.
[21] J.P. Ryckaert, A. Bellemans, Chem. Phys. Lett. 30 (1975) 123–125.
[22] S.H. Lee, J.C. Rasaiah, J. Chem. Phys. 8 (1994) 6964–6974.
[23] W.F. Van Gunsteren, H.J.C. Berendsen, Mol. Phys. 34 (1977) 1311–1327.
[24] H.E. Alper, D. Bassolino, T.R. Stouch, J. Chem. Phys. 12 (1993) 9798–9807.
[25] H.J.C. Berendsen, J.P.M. Postma, W.F. Van Gunsteren, A. DiNola, J.R. Haak, J. Chem. Phys. 8 (1984) 3684–3690.
[26] J.L. Browning, J. Seelig, Biochemistry 19 (1980) 1262–1270.
[27] R.C. MacDonald, S.A. Simon, E. Baer, Biochemistry 4 (1987) 885–891.
[28] P. Yeagle (Ed.), The Structure of Biological Membranes, CRC Press, Boca Raton, 1992.
[29] M.C. Wiener, G.I. King, S.H. White, Biophysical J. 60 (1991) 568–576.
[30] D. Papahadjopoulos, L. Weiss, Biochim. Biophys. Acta 183 (1969) 417–426.
[31] H.E. Alper, D. Bassolino-Klimas, T.R. Stouch, J. Chem. Phys. 99 (1993) 5554–5559.
[32] K. Raghavan, M.R. Reddy, M.L. Berkowitz, Langmuir 8 (1992) 233–240.
[33] A.S. Verkman, A.N. Van Hoek, T. Ma, A. Frigeri, W.R. Skach, A. Mitra, B.K. Tamarappoo, J. Farinas, Water Transport Across Mammalian Cell Membranes. American Physiological Society, 1996, pp. 12–30.
[34] J. Postma, PhD Thesis, Rijkuniversiteit Groningen, The Netherlands, 1985.
[35] N. Takisawa, J. Osugi, M. Nakahara, J. Chem. Phys. 5 (1983) 2591–2597.
[36] M. Nakahara, T. Török, N. Takisawa, J. Osugi, J. Chem. Phys. 10 (1982) 5145–5149.
[37] N. Takisawa, J. Osugi, M. Nakara, J. Phys. Chem. 85 (1981) 3582–3585.
[38] R.W. Impey, P.A. Madden, I.R. McDonald, J. Phys. Chem. 87 (1983) 5071–5083.
[39] M.R. Reddy, M. Berkowitz, J. Chem. Phys. 11 (1988) 7104–7110.
[40] J. Chandrasekhar, D.C. Spellmeyer, W.L. Jorgensen, J. Am. Chem. Soc. 106 (1984) 903–910.